Reaction Kinetics, Mechanisms and Catalysis (2022) 135:2059–2071
https://doi.org/10.1007/s11144-022-02235-5

Catalytic decomposition of H_2O_2 over Nb/KIT-6 catalyst for environmental applications

Gamze Gunduz-Meric[1]

Received: 7 April 2022 / Accepted: 25 May 2022 / Published online: 1 June 2022

Abstract

In this study, it is aimed to investigate catalytic decomposition of hydrogen peroxide for oxygen generation for a fuel-cell based air independent hydrogen production system in underwater applications for our following studies. O_2 and water were generated after H_2O_2 was decomposed catalytically. Here, H_2O_2 acts as an oxidizer and pure O_2 is fed on to a fuel cell and the water is used for hydrolysis reaction of sodium borohydride for clean H_2 production. Due to these reasons, H_2O_2 was selected as an oxygen source concurrently. H_2O_2 is an environmentally friendly chemical because of its decomposition by-product is only water. The prepared Nb based KIT-6 silica catalysts showed high catalytic activities for the H_2O_2 decomposition. These catalysts were characterized by SEM, SEM–EDX, FT-IR, ICP-OES, TEM, N_2 adsorption–desorption and XRD analyses.

Keywords Niobium · KIT-6 · H_2O_2 decomposition · O_2 production · Environmentally-friendly chemical

Introduction

The large specific surface area of KIT-6 is favorable for the dispersion of active metals. This property provides more active sites for the catalytic reaction to KIT-6 based catalysts [1–3]. KIT-6 has three-dimensional pore structure and due to its pore blockage resistance property KIT-6 is an excellent candidate for catalytic applications [4]. Mesoporous KIT-6 silicas have uniform channels, large pore size, high specific area and high thermal stability with its three-dimensional cubic la3d structure [5]. KIT-6, a mesoporous SiO_2 combining the la3d structure to MCM-41 with larger pore diameters and has attracted attention in recent years due to its optimal properties which enhance metal dispersion and accessibility of reactants [6, 7]. Metal dispersion is to adopt new supports like mesostructured silica MCM-41 [8],

✉ Gamze Gunduz-Meric
gamze.gunduz@bilecik.edu.tr

[1] Chemical Engineering Department, Bilecik Seyh Edebali University, 11230 Bilecik, Turkey

SBA-15 [9], KIT-6 [1] etc. with appropriate good thermal and mechanical resistance, large surface area and the well ability to disperse metal active phases to attractive reaction catalysts [10]. Catalyst with high metal dispersion and good durability, many preventive measures have been taken in the catalyst preparation. In this work, Nb was introduced into KIT-6 catalyst. This study was focused on the physicochemical influence of Nb-based catalysts supported on KIT-6 and their catalytic activity in H_2O_2 decomposition. As consequence, they show a relatively high activity for this reaction. Metal into the framework of KIT-6 to achieve stronger solid acid catalyst for organic reactions such as esterification, sucrose hydrolysis, oxidation, epoxidation etc. [11]. In this work, unlike the literature H_2O_2 decomposition reaction was investigated with Nb ions into the mesoporous KIT-6 framework under hydrothermal route. To the knowledge, this is the first time to use the mesoporous silica KIT-6 for this reaction system.

Hydrogen peroxide (H_2O_2) is an environmentally friendly chemical because its only decomposition by-product is water [12–15]. It is a clean oxidant and generally selected as an oxidizer source [16–21]. It is used by many sectors due to its easy access and safe use possibilities [22–24]. It is generally used in waste water treatment or chemical industry [25–27]. However, rare study has focused on its decomposition reaction for O_2 and water generation used in H_2 production. The H_2O_2 decomposition reaction given below [28]:

$$H_2O_2(\text{ads}) \rightarrow 2HO^{\cdot}(\text{ads}) \tag{1}$$

$$H_2O_2(\text{ads}) + HO^{\cdot}(\text{ads}) \rightarrow H_2O\,(\text{ads}) + HO_2^{\cdot}(\text{ads}) \tag{2}$$

$$2HO_2^{\cdot}(\text{ads}) \rightarrow H_2O_2 + O_2 \tag{3}$$

The overall reaction is:

$$H_2O_2 \rightarrow H_2O + \frac{1}{2O_2} \tag{4}$$

This catalytic decomposition process can be performed in not only homogeneous system but also heterogeneous system [29–32]. In recent years, there are some studies that used active metal catalysts for this reaction [32–36]. This reaction also has for long been used for redox catalytic activity of metals [37, 38].

In this study, a catalytic H_2O_2 decomposition reaction was used for generating oxygen and water. Nb monometallic catalysts were synthesized for the hydrogen peroxide decomposition reaction. It was shown that Nb had efficient potential for this reaction. In the following studies it is aimed that the pure oxygen is used as an oxidizer for fuel cell system. The by-product water is stored and used for hydrolysis of sodium borohydride for clean H_2 production [39–42]. It is thought that at these days, O_2 may also plays an important and excellent role. Mesoporous silicas as MCM, SBA, MSU, KIT-6 etc. types have great potentials for many catalytic reactions [8, 9, 43–47]. They are generally used as a catalyst support for chemical reactions and also used for drug delivery, radiotherapy, separation or adsorption

processes [48–51]. This work has focused on Nb based catalysts due to their effective performance in comparison with other active metals [52–54]. The scope of the present study is to demonstrate the suitable and effective metal based catalyst for catalytic H_2O_2 decomposition reaction.

Nb based KIT-6 catalysts with different metal loadings were prepared by hydrothermal method [55]. The catalysts were characterized by X-ray diffraction (XRD), N_2 adsorption–desorption, Transmission electron microscopy (TEM), Fourier transform infrared spectroscopy (FT-IR), Scanning electron microscopy (SEM), energy dispersive X-ray spectroscopy (EDX), inductively coupled plasma-optical emission spectrometry (ICP-OES) analysis. The catalytic performance of the prepared catalysts was evaluated via H_2O_2 catalytic decomposition reaction. Nb based KIT-6 catalysts showed good catalytic performance and especially superior catalytic activity than other supported materials. Catalytic activity for H_2O_2 decomposition with Nb has not been reported as far as we know.

Experimental

Catalyst preparation

Nb based KIT-6 catalysts with different metal contents were prepared by the typical procedure [55]. Nb containing KIT-6 mesoporous la3d structure materials with metal loading 1.5, 3.4, 6.1 and 10.9 wt% were synthesized using Pluronic P123 (Carbosynth) tri-block copolymer and n-butanol (Merck). 5.0 g of P123 was dissolved in 161 ml of 0.5 M hydrochloric acid (Merck) at 35 °C. After dissolution was completed, 5.0 g of n-butanol was added and the resulting mixture was stirred for 1 h at 35 °C. Metal source Niobium (V) chloride (Acros) and the required amounts of TEOS (Abcr) were added to the mixture to obtain the desired molar ratio of 1.5, 3.4, 6.1 and 10.9 wt% and the mixture was stirred for 24 h. Finally, the reaction mixture was poored in a 250 ml Teflon autoclave for hydrothermal treatment (24 h at 100 °C). The final solid was seperated and dried at 100 °C overnight. The directing agent was removed by calcination in dry air at 550 °C for 5 h.

Characterization of catalysts

Surface morphology of Nb loaded KIT-6 catalysts were measured by TEM; JEOL 1220 JEM and SEM using Quanta 400F Field Emission device. FT-IR spectra of all the samples were recorded on Cary 630 Fourier transform infrared spectrometer, equipped with a single reflection diamond attenuated total reflectance (ATR) accessory between 400 and 4000 cm^{-1} employing diluted samples. The textural parameters (specific surface areas, porosities and pore sizes) were obtained via N_2 adsorption–desorption isotherms using BET and BJH methods (Micromeritics ASAP instrument). Before the measurements samples were outgassed at 250 °C and 100 mmHg, overnight. XRD patterns of the samples were obtained by a Panalytical Empyrean instrument at 200 kV and 50 mA with 2θ values ranging between 5° and

80° and with a speed of 10 °C/min. Metal loading were determined from ICP-OES analyses; Perkin Elmer Optima 4300DV.

Catalytic activity tests

0.25 g catalyst was added to an aqueous solution of H_2O_2 (5.5 g, 30%) and the reaction mixture was stirred for 2 h at ambient temperature (~25 °C). At the end of the reaction, the catalyst was separated out. The partly decomposed H_2O_2 was diluted to 250 ml in a standard volumetric flask. Ten milliliter of this solution was transferred in a flask and titrated with standard $KMnO_4$ after addition of 20 ml of 2 M H_2SO_4 and 20 ml water [56]. The decomposition rate of hydrogen peroxide was measured by mass titration with $KMnO_4$. In each reaction experiment, 0.25 g of catalyst was used and four simultaneous reactions were carried out at room temperature.

Results and discussions

Characterization of catalysts

Physical and textural properties of Nb/KIT-6 catalysts were illustrated in Table 1. Results indicated higher surface areas for the catalysts synthesized. An increase in surface area with increasing Nb amount was observed. The increase was due to the increase of porosity emanated from niobium presence resulted in the increase of surface area. The decrease in pore volumes implied incorporation of Nb inside the pores with the increasing Nb amounts on the catalysts. Pore diameters varied between 3.9 and 7.6 nm and these values were determining mesoporous structure (2 nm < pore size < 50 nm). The amount of Nb% loss from the catalyst was determined by ICP-OES analyses (Table 1). Inductively Coupled Plasma (ICP-OES) is an analytical technique in which low concentrations of elements are measured. The sample is sent to argon plasma at a temperature of 6000–10,000 K. In the plasma, molecular bonds are broken, atoms and ions are formed. Immediately after these formed atoms and ions are excited in the plasma, they return to their former energy levels by irradiating at characteristic wavelengths. Emission signals are measured by array detector system. More than one element can be determined at the same time. The determination is made according to the wavelengths depending on the optical properties of the light passed through the plasma. Results indicated a significant loss

Table 1 Textural and physical properties of Nb/KIT-6 catalyst

Catalyst	BET surface area (m^2/g)	Pore volume (cm^3/g)	Pore size (nm)	ICP-OES (Nb% loss)
10.9% Nb/KIT-6	752.5	0.7	3.9	11.8
6.1% Nb/KIT-6	704.2	0.9	6.6	5.2
3.4% Nb/KIT-6	642.2	1.0	7.2	2.4
1.5% Nb/KIT-6	591.6	1.3	7.6	1.2

of active metal synthesized with 10.9% Nb loaded KIT-6 during synthesis. It is seen that the metal loss decreases as the loading ratio decreased. It is thought that the loss occurs during the synthesis procedure or it passed into the washing water during washing procedure.

Wide-angle XRD patterns of Nb containing KIT-6 catalysts prepared with different amounts of metal loading were given in Fig. 1. Small-angle XRD pattern of KIT-6 was at Supplementary file. The peaks of KIT-6 at 2θ of 0.99° and 1.68° indicated the (211) and (220) reflections which are due to the well-ordered cubic 3-D mesoporous arrangement [54]. The broad peak obtained at 23.5° corresponded to amorphous silica. The peaks observed at 2θ values of 34.6°, 37.1°, 48.4°, 51.9°, 58.2°, 62.3°, 68.7°, 70.1°, and 76.4° corresponded to reflections of Nb metal. XRD results are important due to confirming the presence of Nb in the catalyst structure. Similar to the literature, it was observed that the intensity of the peaks increased as the amount of Nb increased [57].

N_2 adsorption–desorption isotherms of catalysts were Type IV according to IUPAC classification which indicated the formation of mesoporous structure with narrow pore size distribution [58]. The KIT-6 has the characteristic type IV isotherm according to the IUPAC classification with an average pore size of 4.5 nm. Nb/KIT-6 catalysts exhibit type II or type IV isotherms with average pore sizes between 4.7 and 5.5 nm (Fig. 2).

Fig. 3 displays the SEM images of the Nb/KIT-6 catalysts. The surface morphology and the spongy nature of Nb/KIT-6 catalysts were investigated. Niobium ions into the catalyst surface affected the smoothness of the materials and Nb/KIT-6 is agglomerated to small irregular particles.

SEM–EDX analysis was also compiled to establish the chemical composition of the Nb/KIT-6. The EDX analysis demonstrated the presence of niobium in Nb/KIT-6

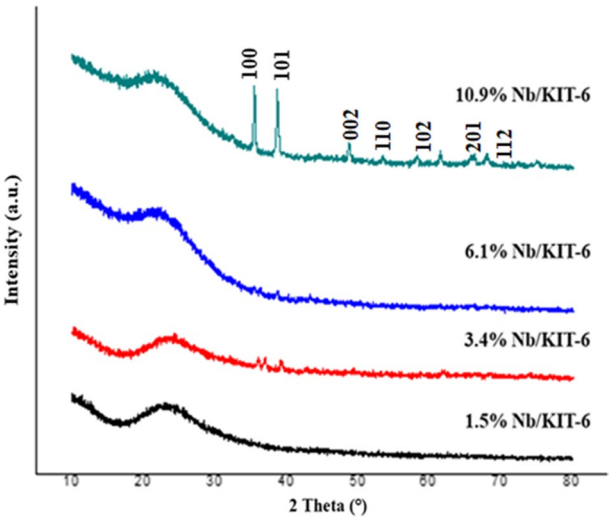

Fig. 1 Wide-angle XRD diffraction patterns of Nb/KIT-6 catalysts [Small-angle XRD diffraction pattern of KIT-6 (Supplementary File)]

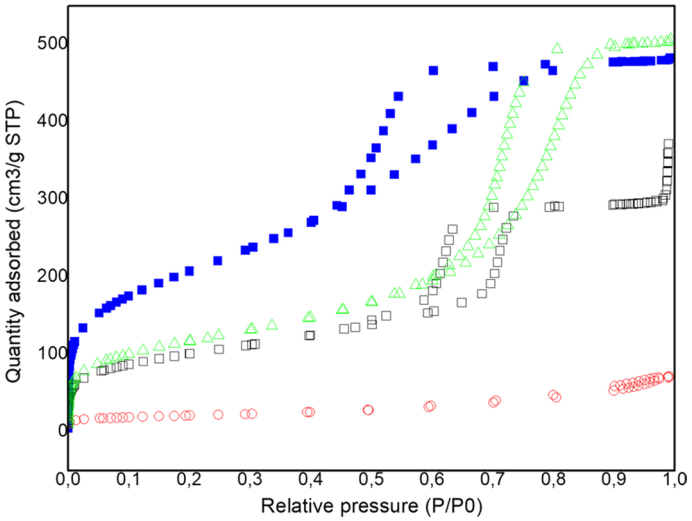

Fig. 2 N_2 adsorption–desorption isotherms of (blue: 10.9%, green: 6.1%, black: 3.4%, red: 1.5%) Nb/KIT-6 catalysts. (Colour figure online)

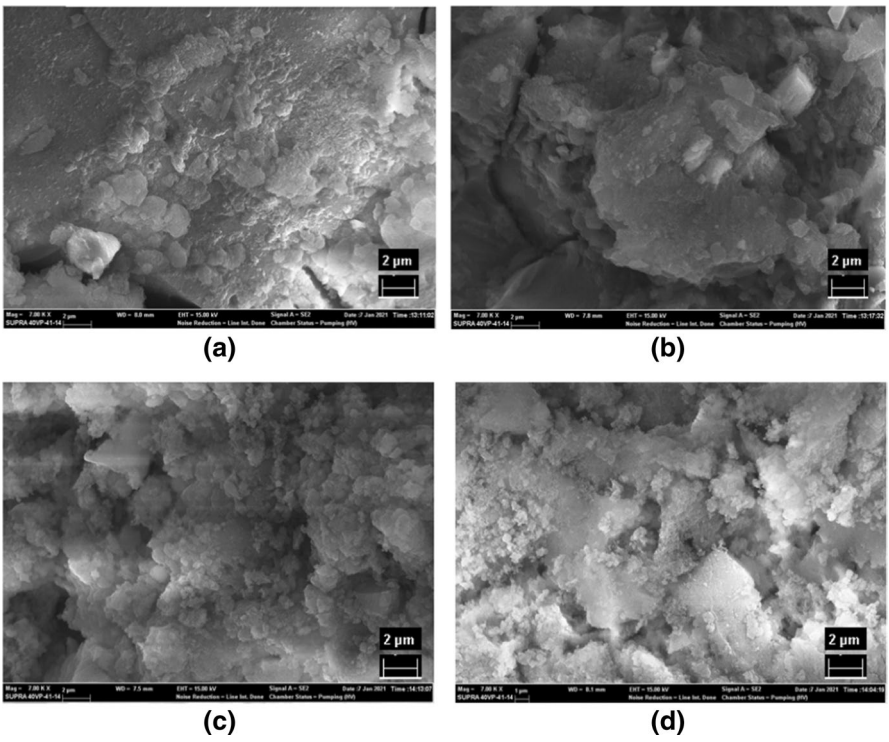

Fig. 3 SEM images of **a** 10.9%, **b** 6.1%, **c** 3.4%, and **d** 1.5% Nb/KIT-6 catalysts (7 KX)

framework. Niobium was successfully incorporated into the KIT-6 mesoporous silica. It was observed from the EDX results that the amount of niobium in the structure increased as the niobium loading rate increased (Supplementary File). The elementel distribution of Nb is indicated using EDX-SEM mapping. Nb particles were homogeneously dispersed on the catalysts surface (Supplementary File).

The morphology of Nb/KIT-6 was also investigated by TEM analysis (Fig. 4). The well-ordered pore structures of mesopores and arrays of mesoporous channels were observed from the images (shown in blue circle).

The FTIR spectra between 400 and 4000 cm^{-1} of Nb/KIT-6 catalysts are shown in Fig. 5. The characteristic peak belonging to Si–O–Si bond appeared at around 1074 cm^{-1} due to symmetric stretching vibrations for all samples. The peaks at 455 cm^{-1} and 806 cm^{-1} corresponded to the bending of Si–O bond and asymmetric bending of Si–O–Si bond, respectively. The symmetric stretching of Si–OH was observed at around 952 cm^{-1}. As well as the band at about 3392 cm^{-1}, the peaks around 1645–1650 cm^{-1} was attributed to –OH stretching vibrations related to adsorbed water molecules which provide surface modification easily [59].

Catalytic performance of the catalysts in decomposition of H_2O_2

All Nb loaded silica based KIT-6 catalysts were tested in decomposition of H_2O_2 reaction. The catalytic activities were observed at room temperature and four simultaneous reactions were carried out for 2 h. In each reaction experiment, 0.25 g of catalyst was used and 4 simultaneous reactions were carried out at room temperature (Run-1 to Run-4). 5.5 g 30% of hydrogen peroxide was used in the reactions and the experiments were carried out in a batch reaction system consisting of a three-necked glass balloon. The amount of hydrogen peroxide decomposed as a result of the reaction was determined as a result of titration of 10 ml samples taken from the reaction mixtures with $KMnO_4$. The reaction was continued for a maximum of 120 min and reaction experiments were carried out under the same experimental conditions at different time intervals. At the end of each reaction, 10 ml of solution was taken and titrated with 0.01 $KMnO_4$ solution according to the procedure applied in the literature [56]. The reaction experiment, which was continued for 120 min, was repeated 4 times, showing that the

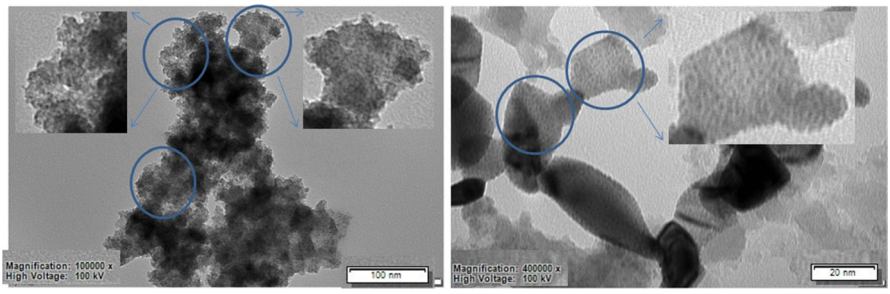

Fig. 4 TEM image of 10.9% Nb/KIT-6 catalyst

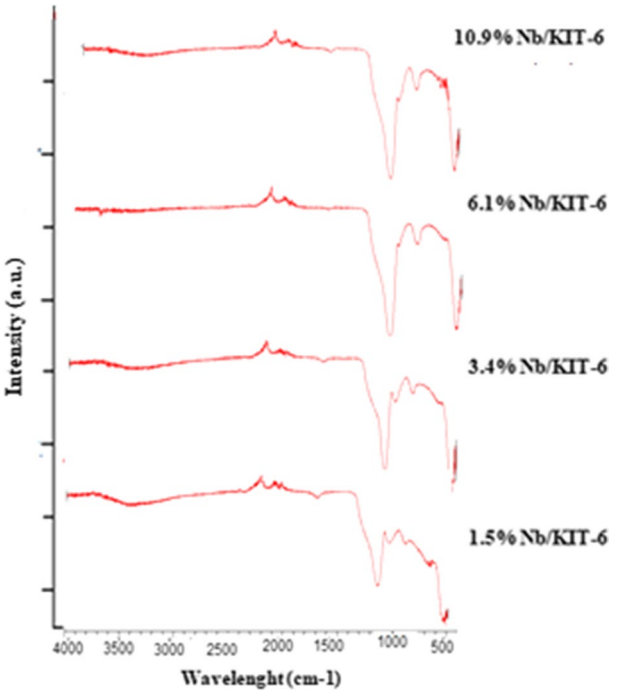

Fig. 5 FT-IR spectra of Nb/KIT-6 catalysts

results were reproducible. The conversion of H_2O_2 after 2 h has shown different trends for all of the catalysts. The decomposition of H_2O_2 is presented in Fig. 6. 0.25 g catalyst was used in the H_2O_2 decomposition reactions carried out to

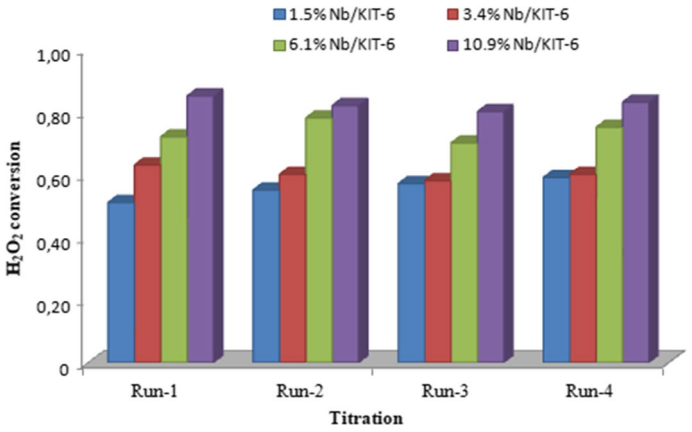

Fig. 6 H_2O_2 conversion over the Nb/KIT-6 catalysts (Reaction conditions: T: ~ 25 °C, t: 2 h, m_{cat}.: 0.25 g with $KMnO_4$ titration and four simultaneous reactions)

determine the catalytic activity and the reactions were carried out in atmospheric pressure at room temperature. Before the reaction experiments, it was observed that H_2O_2 remained intact in the structure at the end of the highest reaction time of 120 min, in the trials without using a catalyst. The experiments carried out for 120 min were repeated 4 times, the conversion values were compared and the reproducibility of the results was examined. In Fig. 6, it was seen that at the end of 120 min, the H_2O_2 conversion reached the highest value of 85% conversion. Experiments performed under the same conditions reveal that the results are reproducible and that the experimental error is negligible. The results showed that the highest conversion value could be reached in a shorter time depending on the amount of active substance added. In other words, the conversion value increases depending on the amount of active substance in the catalyst structure. The results also revealed that the reactant could diffuse into the catalyst during the reaction. For the catalysts, as the niobium loading rate increases, there is a significant increase is observed. The choice of catalyst is justified by the fact that niobium metal is the most successful to catalyze the decomposition of H_2O_2. The catalyst synthesized has shown good activity for H_2O_2 decomposition. There are few studies with metal-containing KIT-6 catalyst in decomposition of H_2O_2 reaction. To the best of knowledge, there is no study about Nb/KIT-6 catalysts in this reaction. Literature survey showed a number of studies regarding to H_2O_2 decomposition. These studies were conducted in the presence of different variety of metal containing catalysts and varying experimental conditions (Table 2). It is clearly observed from the table that these Nb/KIT-6 catalysts exhibit the highest activity and efficiency. The Nb/KIT-6 catalyst synthesized in this study has shown good activity for H_2O_2 decomposition reaction. A comparison with literature must be made in order to better visualize the extent of its activity and efficiency. Literature survey showed a few and new number of studies regarding to H_2O_2 decomposition reaction with KIT-6 catalysts. These studies were conducted in the presence of a variety of catalysts with varying experimental conditions and selected studies were summarized. It was clearly seen from the table that synthesized catalyst had been among the ones with highest activity and efficiency [56, 60–62]. It is obvious from reaction experiments and characterization analyses

Table 2 Literature comparison of the catalysts in H_2O_2 decomposition

References	Catalyst	Reaction conditions	Conversion
[56]	M-Y zeolite (M: Cr, Fe, Bi, Ni, and Zn)	T: ~ 25 °C, t: 1–2 h, 0.025 g cat	Max. 45.69% H_2O_2 with Fe-Y (2 h)
[60]	Rh/Au BNPs	T: 25 °C	600 mol-H_2O_2 min^{-1} mol-M^{-1} (with UV–Vis spectra)
[61]	CNTs	T: 25 °C, 0.05 g cat	10% H_2O_2 (30 min)
[62]	CN-S, CN-N	T: 25 °C, t: 1 h, 50 mg cat	Degredation rate constant: 0.0508 min^{-1}
This work	Nb/KIT-6	T:25 °C, t:2 h, 0.25 g cat	Max. 85% H_2O_2 (10.9% Nb)

that 10.9% Nb/KIT-6 catalyst had the highest activity among those synthesized by varying Nb amounts. This was among the most important results of the present study as it showed the possibility of a sustainable production.

Reaction experiments conducted in the order of 10.9% Nb (85%) > 6.1% Nb (72%) > 3.4% Nb (63%) > 1.5% (51%) Nb/KIT-6 based on H_2O_2 conversion. From reaction experiments and characterization studies it is obvious that 10.9% Nb/KIT-6 catalyst had the highest activity (85% H_2O_2 conversion) among those synthesized by varying Nb amounts. It was seen that as the amount of Nb increased, the activity increased accordingly. Nb was among the proper choices with its efficient property in this reaction.

Conclusions

Nb/KIT-6 with different Si/Nb weight ratios was successfully synthesized. The presence of highly ordered structure was evident from SEM, SEM–EDX, TEM and N_2 adsorption–desorption analysis. The absence of Nb crystals was inferred from XRD spectra. The effects of varying Nb amounts on the catalytic properties of KIT-6 catalysts were investigated during H_2O_2 decomposition at 25 °C. Nb based KIT-6 catalysts presented high activity. Catalytic tests and characterization studies revealed better performance. It is noteworthy that the catalytic activity of Nb/KIT-6 was increased with increasing amounts of niobium. In this study, where the catalytic activity was investigated by the H_2O_2 decomposition reaction, the results showed that the reactant could diffuse into the catalyst and the conversion value increased according to the increasing amount of active substance in the catalyst structure. The obtained high catalytic activity revealed that the catalyst is an important alternative for such reactions. This shows that niobium is an effective metal for this reaction. There is no previous study in the literature using this metal in this reaction. Nb-containing mesoporous silicas have attracted good consideration as catalysts in similar reactions. Nb into the KIT-6 structure generated better Lewis and Bronsted acid sites this is why it was chosen for this reaction. In the following studies it is aimed that the pure oxygen is used as an oxidizer for fuel cell system and the by-product water is used for hydrolysis of sodium borohydride for clean H_2 production with a systematic reaction process.

Supplementary Information The online version contains supplementary material available at https://doi.org/10.1007/s11144-022-02235-5.

Acknowledgements Bilecik Seyh Edebali University, Yıldız Technical University and Eskisehir Osmangazi University Central Research Laboratories are gratefully acknowledged for characterization studies. Part of the study was supported by the BAP 2019-02.BŞEÜ.03-04 project.

Declarations

Conflict of interest The author declares that they have no known competing financial interest or personal relationships that could have appeared to influence the work reported in this paper.

References

1. Lv Y, Xin Z, Meng X, Tao M, Bian Z, Gu J, Gao W (2017) Effect of La, Mg and Mo additives on dispersion and thermostability of Ni species on KIT-6 for CO methanation. Appl Catal A 543:125–132
2. Bérubé F, Kaliaguine S (2008) Calcination and thermal degradation mechanisms of triblock copolymer template in SBA-15 materials. Microporous Mesoporous Mater 115(3):469–479
3. Mandal M, Kruk M (2012) Surfactant-templated synthesis of ordered silicas with closed cylindrical mesopores. Chem Mater 24(1):149–154
4. Kishor R, Ghoshal AK (2017) Understanding the hydrothermal, thermal, mechanical and hydrolytic stability of mesoporous KIT-6: a comprehensive study. Microporous Mesoporous Mater 242:127–135
5. Vinu A, Gokulakrishnan N, Balasubramanian VV, Alam S, Kapoor MP, Ariga K, Mori T (2008) Three-dimensional ultralarge-pore Ia3d mesoporous silica with various pore diameters and their application in biomolecule immobilization. Chem A Eur J 14(36):11529–11538
6. Wu S, Lan P (2012) A kinetic model of nano-CaO reactions with CO_2 in a sorption complex catalyst. AlChE J 58:1570–1577
7. Broda M, Kierzkowska AM, Baudouin D et al (2012) Sorbent-enhanced methane reforming over a Ni-Ca based, bifunctional catalyst sorbent. ACS Catal 2:1635–1646
8. Zhang J, Xin Z, Meng X, Lv Y, Tao M (2014) Effect of MoO_3 on the heat resistant performances of nickel based MCM-41 methanation catalysts. Fuel 116:25–33
9. Bian Z, Meng X, Tao M, Lv Y, Xin Z (2016) Uniform Ni particles on amino-functionalized SBA-16 with excellent activity and stability for syngas methanation. J Mol Catal A Chem 417:184–191
10. García-Sancho C, Moreno-Tost R, Mérida-Robles JM, Santamaría-González J, Jiménez-López A, Maireles-Torres P (2011) Niobium-containing MCM-41 silica catalysts for biodiesel production. Appl Catal B 108:161–167
11. Anilkumar M, Hoelderich WF (2015) A one step synthesis ofcaprolactam out of cyclohexanone by combinded ammoximation and Beckmann rearrangement over Nb-MCM-41 catalysts. Appl Catal B 165:87–93
12. Gudarzi D, Ratchananusorn W, Turunen I, Heinonen M (2015) Factors affecting catalytic destruction of H_2O_2 by hydrogenation and decomposition over Pd catalysts supported on activated carbon cloth (ACC). Catal Today 248:69–79
13. Wang Y, Guo Z, Xia Y (2013) A thin-film direct hydrogen peroxide/borohydride micro fuel cell. Adv Energy Mater 3(6):713–717
14. Zaki MI, Katrib A, Muftah AI, Jagadale TC, Ikram M, Ogale SB (2013) Exploring anatase-TiO_2 doped dilutely with transition metal ions as nano-catalyst for H_2O_2 decomposition: Spectroscopic and kinetic studies. Appl Catal A 452:214–221
15. Amirfakhri SJ, Binny D, Meunier JL, Berk D (2014) Investigation of hydrogen peroxide reduction reaction on graphene and nitrogen doped graphene nanoflakes in neutral solution. J Power Sources 257:356–363
16. Yi Y, Wang L, Li G, Guo H (2016) A review on research progress in the direct synthesis of hydrogen peroxide from hydrogen and oxygen: noble-metal catalytic method, fuel-cell method and plasma method. Catal Sci Technol 6(6):1593–1610
17. Mase K, Yoneda M, Yamada Y, Fukuzumi S (2016) Seawater usable for production and consumption of hydrogen peroxide as a solar fuel. Nat Commun 7(1):1–7
18. Moon GH, Fujitsuka M, Kim S, Majima T, Wang X, Choi W (2017) Eco-friendly photochemical production of H_2O_2 through O_2 reduction over carbon nitride frameworks incorporated with multiple heteroelements. ACS Catal 7(4):2886–2895
19. Kim HI, Kwon OS, Kim S, Choi W, Kim JH (2016) Harnessing low energy photons (635nm) for the production of H_2O_2 using up conversion nanohybrid photocatalysts. Energy Environ Sci 9(3):1063–1073
20. Shiraishi Y, Kofuji Y, Sakamoto H, Tanaka S, Ichikawa S, Hirai T (2015) Effects of surface defects on photocatalytic H_2O_2 production by mesoporous graphitic carbon nitride under visible light irradiation. ACS Catal 5(5):3058–3066
21. Song H, Wei L, Chen C, Wen C, Han F (2019) Photocatalytic production of H_2O_2 and its in situ utilization over atomic-scale Au modified MoS_2 nanosheets. J Catal 376:198–208

22. Liu X, Zhu T, Lv Q, Li Y, Che D (2019) Simultaneous removal of NOx and SO_2 from coal-fired flue gas based on the catalytic decomposition of H_2O_2 over $Fe_2(MoO_4)_3$. Chem Eng J 371:486–499
23. Qi Y, Ge P, Wang M, Shan X, Ma R, Huang J, Wu J (2020) Experimental investigation and numerical simulation of simultaneous desulfurization and denitrification by H_2O_2 solution assisted with microwave and additive. Chem Eng J 391:123559
24. Yang B, Ma S, Cui R, Sun S, Wang J, Li S (2019) Simultaneous removal of NO_x and SO_2 with H_2O_2 catalyzed by alkali/magnetism-modified fly ash: high efficiency, low cost and catalytic mechanism. Chem Eng J 359:233–243
25. Anilkumar M, Hoelderich WF (2012) Gas phase Beckmann rearrangement of cyclohexanone oxime to ε-caprolactam over mesoporous, microporous and amorphous Nb_2O_5/silica catalysts: a comparative study. Catal Today 198(1):289–299
26. Yan W, Ramanathan A, Patel PD, Maiti SK, Laird BB, Thompson WH, Subramaniam B (2016) Mechanistic insights for enhancing activity and stability of Nb-incorporated silicates for selective ethylene epoxidation. J Catal 336:75–84
27. Thornburg NE, Nauert SL, Thompson AB, Notestein JM (2016) Synthesis−structure–function relationships of silica-supported niobium (V) catalysts for alkene epoxidation with H_2O_2. ACS Catal 6(9):6124–6134
28. Hiroki A, LaVerne JA (2005) Decomposition of hydrogen peroxide at water− ceramic oxide interfaces. J Phys Chem B 109(8):3364–3370
29. Dong C, Ji J, Shen B, Xing M, Zhang J (2018) Enhancement of H_2O_2 decomposition by the co-catalytic effect of WS_2 on the Fenton reaction for the synchronous reduction of Cr (VI) and remediation of phenol. Environ Sci Technol 52(19):11297–11308
30. Ma C, Feng S, Zhou J, Chen R, Wei Y, Liu H, Wang S (2019) Enhancement of H_2O_2 decomposition efficiency by the co-catalytic effect of iron phosphide on the Fenton reaction for the degradation of methylene blue. Appl Catal B 259:118015
31. Gunduz-Meric G (2021) Fe/KIT-6 Katalizörlerinin Sentezi, Karakterizasyonu ve H_2O_2 Bozunma Reaksiyonunda Aktivitelerinin İncelenmesi. Afyon Kocatepe Üniv Fen ve Mühendis Bilim Derg 2021(2):442–448
32. Gunduz G, Degirmenci L (2016) Silika ile Mikroenkapsüle Edilmiş Fe_2O_3 İçerikli Kürelerin Üretim Prosesinin İyileştirilmesi ve Katalitik Aktivitelerinin Belirlenmesi. Gazi Üniv Mühendis Mimar Fakültesi Derg. https://doi.org/10.17341/gummfd.84263
33. Ali N, Zaman H, Bilal M, Nazir MS, Iqbal HM (2019) Environmental perspectives of interfacially active and magnetically recoverable composite materials—a review. Sci Total Environ 670:523–538
34. Ji X, Han Z, Li J, Deng Y, Han X, Zhao J et al (2019) MoSx co-catalytic activation of H_2O_2 by heterogeneous hemin catalyst under visible light irradiation. J Colloid Interface Sci 557:301–310
35. Xing M, Xu W, Dong C, Bai Y, Zeng J, Zhou Y et al (2018) Metal sulfides as excellent co-catalysts for H_2O_2 decomposition in advanced oxidation processes. Chem 4(6):1359–1372
36. Luo H, Cheng Y, Zeng Y, Luo K, Pan X (2020) Enhanced decomposition of H_2O_2 by molybdenum disulfide in a Fenton-like process for abatement of organic micropollutants. Sci Total Environ 732:139335
37. Spear EB (1908) Catalytic decomposition of hydrogen peroxide under high pressures of oxygen. 2. J Am Chem Soc 30(2):195–209
38. Satterfield C, Stein T (1957) Decomposition of hydrogen peroxide vapor on relatively inert surfaces. Ind Eng Chem 49(7):1173–1180
39. Park T, Chang I, Jung JH, Lee HB, Ko SH, O'Hayre R et al (2017) Effect of assembly pressure on the performance of a bendable polymer electrolyte fuel cell based on a silver nanowire current collector. Energy 134:412–419
40. Kim T (2009) Micro methanol reformer combined with a catalytic combustor for a PEM fuel cell. Int J Hydrogen Energy 34(16):6790–6798
41. Joh HI, Ha TJ, Hwang SY, Kim JH, Chae SH, Cho JH et al (2010) A direct methanol fuel cell system to power a humanoid robot. J Power Sources 195(1):293–298
42. Schlesinger HI, Brown HC, Finholt AE, Gilbreath JR, Hoekstra HR, Hyde EK (1953) Sodium borohydride, its hydrolysis and its use as a reducing agent and in the generation of hydrogen1. J Am Chem Soc 75(1):215–219
43. He Q, Shi J, Cui X, Zhao J, Chen Y, Zhou J (2009) Rhodamine B-co-condensed spherical SBA-15 nanoparticles: facile co-condensation synthesis and excellent fluorescence features. J Mater Chem 19(21):3395–3403

44. Kim TW, Kleitz F, Paul B, Ryoo R (2005) MCM-48-like large mesoporous silicas with tailored pore structure: facile synthesis domain in a ternary triblock copolymer− butanol−water system. J Am Chem Soc 127(20):7601–7610
45. Park DH, Kim SS, Pinnavaia TJ, Tzompantzi F, Prince J, Valente JS (2011) Selective isobutene oligomerization by mesoporous MSU-S_{BEA} catalysts. J Phys Chem C 115(13):5809–5816
46. Shen S, Chen J, Koodali RT, Hu Y, Xiao Q, Zhou J et al (2014) Activation of MCM-41 mesoporous silica by transition-metal incorporation for photocatalytic hydrogen production. Appl Catal B 150:138–146
47. Prathap MA, Kaur B, Srivastava R (2012) Direct synthesis of metal oxide incorporated mesoporous SBA-15, and their applications in non-enzymatic sensing of glucose. J Colloid Interface Sci 381(1):143–151
48. Pirez C, Caderon JM, Dacquin JP, Lee AF, Wilson K (2012) Tunable KIT-6 mesoporous sulfonic acid catalysts for fatty acid esterification. ACS Catal 2(8):1607–1614
49. Xia Y, Yang Z, Mokaya R (2004) Mesostructured hollow spheres of graphitic N-doped carbon nanocast from spherical mesoporous silica. J Phys Chem B 108(50):19293–19298
50. Argyo C, Weiss V, Bräuchle C, Bein T (2014) Multifunctional mesoporous silica nanoparticles as a universal platform for drug delivery. Chem Mater 26(1):435–451
51. Kong L, Mume E, Triani G, Smith SV (2013) Optimizing radiolabeling amine-functionalized silica nanoparticles using SarAr-NCS for applications in imaging and radiotherapy. Langmuir 29(18):5609–5616
52. Wang W, Qi R, Shan W, Wang X, Ji Q, Zhao J et al (2014) Synthesis of KIT-6 type mesoporous silicas with tunable pore sizes, wall thickness and particle sizes via the partitioned cooperative self-assembly process. Microporous Mesoporous Mater 194:167–173
53. Ramanathan A, Subramaniam B, Maheswari R, Hanefeld U (2013) Synthesis and characterization of Zirconium incorporated ultra large pore mesoporous silicate, Zr–KIT-6. Microporous Mesoporous Mater 167:207–212
54. Ramanathan A, Maheswari R, Barich DH, Subramaniam B (2014) Niobium incorporated mesoporous silicate, Nb-KIT-6: synthesis and characterization. Microporous Mesoporous Mater 190:240–247
55. Ghohe NM, Tayebee R, Amini MM (2019) Synthesis and characterization of mesoporous Nb-Zr/KIT-6 as a productive catalyst for the synthesis of benzylpyrazolyl coumarins. Mater Chem Phys 223:268–276
56. Maurya MR, Titinchi SJJ, Chand S, Mishra IM (2002) Zeolite-encapsulated Cr (III), Fe (III), Ni (II), Zn (II) and Bi (III) salpn complexes as catalysts for the decomposition of H_2O_2 and oxidation of phenol. J Mol Catal A Chem 180(1–2):201–209
57. Bermúdez JM, Arenillas A, Menéndez JA (2011) Syngas from CO_2 reforming of coke oven gas: synergetic effect of activated carbon/Ni–γAl_2O_3 catalyst. Int J Hydrogen Energy 36:13361–13368
58. Sing KS (1985) Reporting physisorption data for gas/solid systems with special reference to the determination of surface area and porosity (Recommendations 1984). Pure Appl Chem 57(4):603–619
59. Xu L, Wang C, Guan J (2014) Preparation of acid-base bifunctional mesoporous KIT-6 (KIT: Korea Advanced Institute of Science and Technology) and its catalytic performance in Knoevenagel reaction. J Solid State Chem 213:250–255
60. Zhang H, Deng X, Jiao C, Lu L, Zhang S (2016) Preparation and catalytic activities for H_2O_2 decomposition of Rh/Au bimetallic nanoparticles. Mater Res Bull 79:29–35
61. Voitko K, Tóth A, Demianenko E, Dobos G, Berke B, Bakalinska O et al (2015) Catalytic performance of carbon nanotubes in H_2O_2 decomposition: experimental and quantum chemical study. J Colloid Interface Sci 437:283–290
62. Wang X, Li D, Nan Z (2019) Effect of N content in g-C_3N_4 as metal-free catalyst on H_2O_2 decomposition for MB degradation. Sep Purif Technol 224:152–162